

# Single End-Fire Antenna for Dual-Beam and Broad Beamwidth Operation at 60 GHz by artificially modifying the Permittivity of the Antenna substrate

Abdolmehdi Dadgarpour, Behnam Zarghooni, Bal S. Virdee, and Tayeb A. Denidni

**Abstract**— A technique is proposed to generate a dual-beam and broad beamwidth radiation in the E-plane of a printed bow-tie antenna operating over 57–64 GHz. This is achieved by artificially modifying the dielectric constant of the antenna substrate using arrays of metamaterial inclusions realized using stub-loaded H-shaped unit-cells to provide a high index of refraction. The H-shaped inclusions are tilted with respect to the axis of the antenna and embedded in the direction of the end-fire radiation. The resulting dual-beam radiation in the E-plane has maxima at +60 and 120 degrees with respect to the end-fire direction (90 degrees) with a maximum peak gain of 9 dBi at 60 GHz.

**Index Terms**—Dual-beam, broad beamwidth, antenna, bow-tie antenna, millimeter-wave antennas, 5G wireless networks.

## I. INTRODUCTION

Recently, the work at millimeter-wave frequency band, in particular at 60 GHz, has attracted great attention by researchers as this band offers transmission rates of multi-gigabits per second, which is necessary for applications requiring video streaming and Internet-of-Things (IoT)/Machine-to-Machine (M2M) communications to be implemented in 5G wireless networks [1],[2].

Working at this frequency band is particularly challenging because the quality of the communication link is degraded by: (i) substantial loss due to atmospheric absorption, (ii) interference effect from adjacent channels, (iii) multipath effect causing signal fading, and (iv) link blockage by obstructions. Loss can be compensated by using high-gain antennas. In order to overcome the interference effect and where coverage of multiple non-adjacent areas is required it is necessary to employ multi-beam antennas. Such antennas confine the power in specific directions instead of scattering the power everywhere. In [3] improved spatial diversity is demonstrated with dual-beam MIMO compared to classical MIMO, where power gain of 1.6 dB is achieved at 60 GHz band. Authors in [4][5] have shown that by employing a dual-beam antenna at the transmitter and receiver improve the link quality where the link blockage is encountered due to multipath effect and mutual interference. Dual-beam antennas that radiate energy symmetrically at two different angles also find application in scanning and millimeter-wave identification (MMID) systems [6]-[8].

Various types of antennas with different functionalities have been studied at millimeter-wave frequencies. For instance, end-fire radiating antennas, such as Yagi-Uda, dipole, as well as bow-tie, have been widely reported for millimeter-wave frequency band applications, in particular, beam switching networks, beam tilting and beam steering [9]-[16].

One approach to generate multiple beams or dual-beams is to employ antenna arrays with adaptive radiation pattern using phased array antennas [17]. To implement this technique requires multiple antenna arrays as well as phase shifters, which makes this approach costly and requiring a larger

footprint size. To overcome these limitations, the authors in [18] have utilized gradient index of refraction media in the classical dipole antenna. By switching the appropriate feed-line in the antenna structure, the direction of the main beam can be steered towards one of two specific angles. To achieve multiple beams with this technique requires electronically controlled SPDT switches, which can introduce extra loss and complexity into the system.

Pattern reconfigurability is another promising technique reported in [19] where EBG structures are placed symmetrically around the 60 GHz antenna to achieve beam steering by meanings of switching diodes ‘on’ or ‘off’. Although the radiation pattern of the antenna can be steered at discrete angles in the azimuth plane the diodes introduce extra loss and complexity into the system.

Extensive investigation has been carried out to obtain dual-beam radiation pattern using leaky wave antennas [20]-[24]. The drawback of these antennas is the dual-beam radiation pattern is affected by the frequency, which restricts its applications. To overcome this limitation, the authors in [25] have excited higher  $TM_{02}$  mode in a U-slot patch antenna to realize a dual-beam with a wide beamwidth. Even though the radiation beam is fixed over the antenna’s operating frequency range of 5.18–5.8 GHz, the antenna gain is relatively low for practical applications.

In this paper, a technique is proposed to realize a dual-beam antenna for millimeter-wave applications over 57–64 GHz. This is realized on an end-fire bow-tie antenna by incorporating metamaterial inclusions which are implemented with stub-loaded H-shaped unit-cells. The array of  $4 \times 4$  inclusions are tilted with respect to the end-fire direction. Reduction in the back-lobe radiation and enhancement of the antenna gain is achieved by loading a pair of H-shaped resonators next to the feed-line near the bow-tie radiators. To improve the coverage of the communications link over the designated area it is necessary to widen the beamwidth of the antenna, which is particularly challenging at 60 GHz band [26]. We have broadened the 3 dB beamwidth of the antenna by including an array of non-tilted  $2 \times 3$  inclusions in the end-fire direction of the bow-tie radiators. The measured reflection coefficient of the antenna is better than -10 dB over 57–64 GHz and the two radiation beams generated point at angles of 60 and 120 degrees with respect to the end-fire direction (90 degrees) with maximum peak realized gain of 9 dBi. These properties make such an antenna suitable for improving the communications link of systems effected by multipath effect and mutual interference [4][5], and in scanning and MMID applications [6]-[8]. In our previous work [18] we have employed gradient index of refraction with multiple dipole antennas with switches to generate dual-beam radiation, where the beam deflection is limited to angles  $+26^\circ$  and  $-26^\circ$ . By exciting individual antennas separately using SP4T switches we are able to generate dual-beam radiation which is limited to angles  $+26^\circ$  and  $-26^\circ$  with respect to the end-fire direction.

However, as can be observed in Fig. 18 of [18] we are unable to achieve dual-beam when both feeds are excited simultaneously, in which case a single main beam is created that radiates in the end-fire direction.

## II. MECHANISM OF DUAL-BEAM

Here dual-beam radiation is established by exploiting the dielectric slab mode TE in the printed bow-tie dipole antenna as described in [27][28]. To excite TE surface modes it is necessary to utilize high dielectric constant substrates [29]. It is well known that a high dielectric constant substrate can adversely affect the antenna's radiation efficiency and gain performance as the electromagnetic energy is confined within the substrate. Hence the bow-tie antenna used here was designed on a low dielectric constant substrate (RO5880) with relative dielectric constant of 2.2.

When excited the printed bow-tie antenna launches TE surface waves and the resulting radiation emanating from the antenna is tailored to point towards a predefined angle by creating a region of high refractive index on the antenna. This was achieved by embedding metamaterial unit-cell inclusions described by the authors in [18]. Integration of metamaterial inclusions on the RO5880 substrate was designed to artificially increase the effective dielectric constant of the substrate in order to refract the electromagnetic radiation from the bow-tie antenna. This technique was implemented here by using an array of stub-loaded H-shaped electric resonators or unit-cells depicted in Fig. 1.

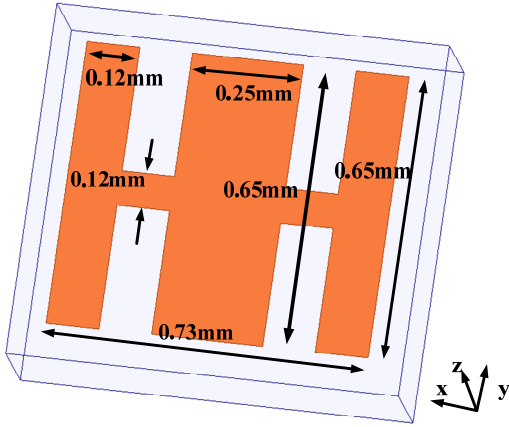


Fig. 1. Geometry of the proposed H-shaped metamaterial unit-cell fabricated on the dielectric substrate (RO5880).

The unit-cell's intrinsic parameters were extracted using HFSS software tools by locating the PEC and PMC boundary conditions in the  $yz$ - and  $xy$ -planes with the two wave ports arranged along the  $y$ -direction [30]. Hence when the electric-field is polarized in optical axis of the proposed unit-cell in the  $x$ -direction, the electric resonance is generated, and the proposed unit-cell can be regarded as an  $LC$  resonator. Fig. 2 shows that the real part of permittivity varies from 3.2–7.3 over the frequency range 57–64 GHz. The operational region of the unit-cell needs to be far-way from its resonant frequency to minimise loss. The corresponding refractive-index varies from 1.81–2.22, which is larger than antenna substrate with effective refractive-index value of 1.28. Hence

by embedding the proposed unit-cells in front of end-fire radiation will cause the antenna to excite surface waves whose phase velocity is lower than the phase velocity of the waves in the substrate, thus altering the direction of the radiation.

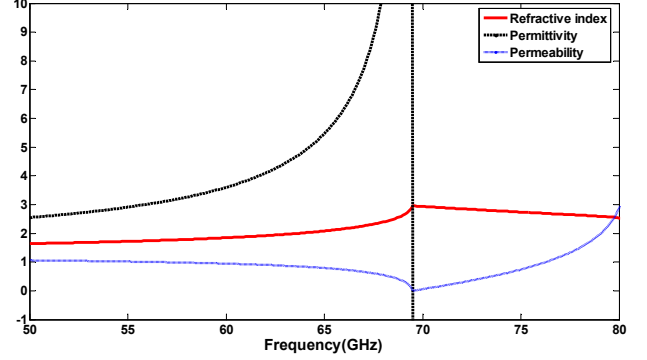


Fig. 2. The extracted characterizing parameters of proposed unit-cell including permittivity, permeability and refractive index.

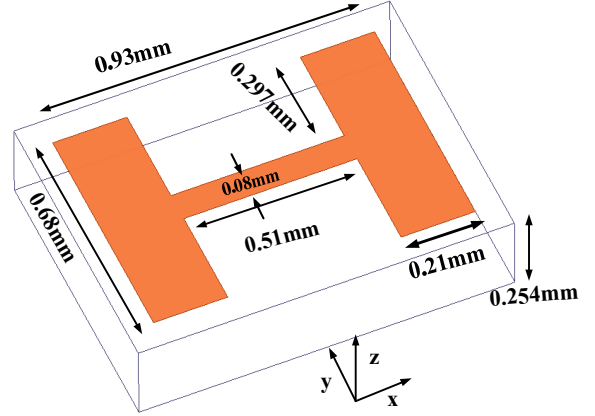


Fig. 3. The structure of the H-shaped unit-cell.

In order to improve the gain of the antenna and reduce its back-lobe radiation a pair of H-shaped resonators, shown in Fig. 3, was loaded onto the antenna. The S-parameter response of the resonator was obtained by exciting the two wave ports in the  $y$ -direction in order to induce electric and magnetic fields in the  $x$ - and  $z$ -directions, respectively. The transmission coefficient response of proposed structure in Fig. 4 indicates that it has a band-stop response over 57–64 GHz. In Section III, it is shown that by integrating the proposed H-shaped resonators at the back side of end-fire antenna results in the suppression of backward surface waves that are reflected at the edge of ground-plane [16].

## III. DUAL-BEAM RADIATION PATTERN IN THE AZIMUTH PLANE

The proposed antenna, shown in Fig. 5, comprises printed bow-tie radiators constructed on Rogers 5880 substrate with relative dielectric constant 2.2 and thickness 0.254 mm. The bow-tie radiators are fed by microstrip lines that are tapered at its end to improve its impedance match. The antenna is loaded with two H-shaped resonators next to the feed-line and just below the bow-tie radiators to minimize the back-lobe and

side radiation. Fig. 6 shows these unit-cells effectively enhance the antenna gain by 2.66 dB from 4.1 dBi to 6.76 dBi.

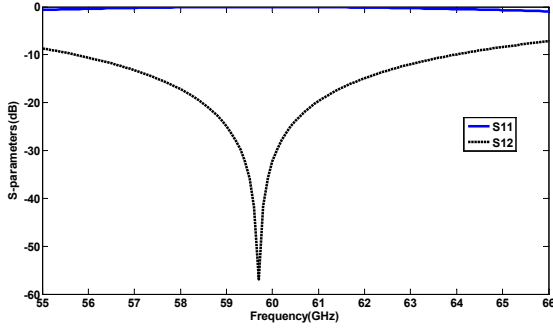


Fig. 4. S-parameter ( $S_{12}$  and  $S_{11}$ ) response of the H-shaped configuration.

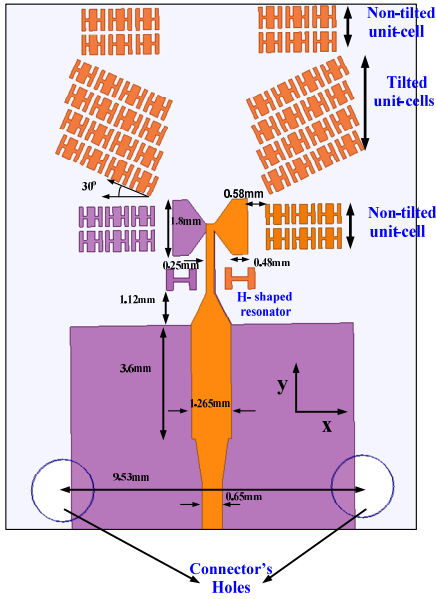


Fig. 5. Configuration of the antenna embedded with a  $3 \times 4$  array of the proposed HRIM unit-cells on upper surface of antenna substrate.

Embedded in the antenna include arrays of non-tilted stub-loaded H-shaped unit-cells placed along the  $x$ -direction of bow-tie antenna, as shown in Fig. 5, whose purpose is broaden its beamwidth. It can be observed in Fig. 6 that by loading the antenna with non-tilted unit-cells contributes in increasing the 3 dB beamwidth of the bow-tie antenna by 67 degrees from 53 to 120 degrees compared to conventional bow-tie antenna with 3 dB beamwidth of 53 degrees ( $62^\circ$ – $115^\circ$ ). This property can be used for providing a broader coverage for wireless communications over 57–64 GHz. It means that we have a radiation at 53 and 120 degrees with respect to the end-fire direction (90 degrees) compared to conventional bow-tie antenna as revealed in Fig. 6. Thus, we can generate a dual-beam radiation by embedding onto the antenna unit-cells that are tilted by 30 degrees with respect to the antenna's axis. The reason why we have tilted proposed unit-cells by 30 degrees is attributed to the increase of the 3dB beamwidth of antenna by  $67/2=33$  degrees in each direction with respect to the

antenna's axis. Thus, we can obtain a larger steer angle by simply increasing the 3dB beamwidth more than 67 degrees.

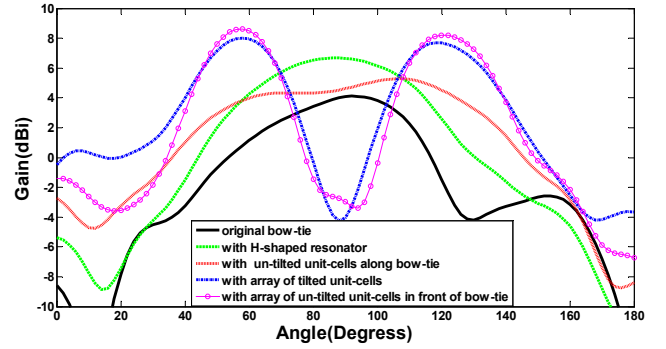


Fig. 6. The radiation pattern of antenna in the E-plane with different arrangement of tilted and non-tilted unit-cells at 60 GHz.

As mentioned in Section II, in order to excite TE surface waves it is necessary to integrate a higher refractive index medium in the end-fire region of the bow-tie antenna. This is achieved here by artificially creating a higher index of refraction using an array of stub-loaded H-shaped unit-cells that exhibit a higher effective permittivity and refractive index than antenna substrate as is evident in Fig. 2. In particular, the  $4 \times 4$  arrays of stub-loaded H-shaped unit-cells were integrated in the end-fire direction ( $y$ -axis) of the bow-tie radiators, as shown in Fig. 5. The  $4 \times 4$  arrays are tilted by 30 degrees with respect to the end-fire direction. The result of this arrangement, shown in Fig. 6, reveals that at 60 GHz the dual-beam radiation pattern is created with maximum peak gain of 7.9 dBi at  $60^\circ$  and  $120^\circ$  with respect to end-fire radiation (90 degrees). By introducing another  $2 \times 3$  array of non-tilted stub-loaded H-shaped unit-cells in front of the tilted unit-cells enhance the antenna gain by 1 dBi. Furthermore, the  $2 \times 3$  array reduces the side-lobe level by almost 4 dB.

To better exemplify the effect of H-shaped inclusions on the antenna, the radiation pattern of the original bow-tie antenna with and without H-shaped resonators is plotted in Fig. 7. It can be observed that by embedding the H-shaped resonators on the back side of bow-tie antenna results in the improvement of back-lobe radiation by about 5 dB in the H-plane. This leads to gain enhancement in the end-fire direction compared with original bow-tie, as shown in Fig. 6.

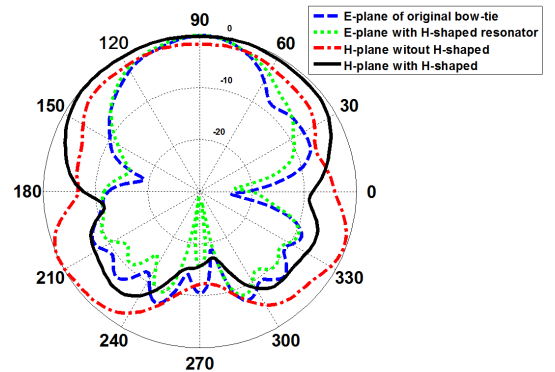


Fig. 7. The E- and H-plane radiation patterns of the bow-tie antenna with and without H-shaped resonators.

The TE mode surface waves were excited by artificially creating a high dielectric constant region in the end-fire vicinity of the bow-tie antenna by embedding arrays of stub-loaded H-shaped unit-cells. To validate the approach undertaken high dielectric constant substrates with permittivity of 4 and 6 were integrated into the antenna substrate, as shown in Fig. 8. The antenna substrate had permittivity of 2.2. The result of this study in Fig. 9 show that when a substrate with dielectric constant 4 was used the antenna exhibits dual-beam radiation in the azimuth plane at 60 and 120 degrees with maximum gain of about 7 dBi, which is analogous to loading the antenna with artificial metamaterial inclusions. When a substrate with dielectric constant 6 is used the antenna radiates dual-beam at 50 and 130 degrees with maximum gain of 7 dBi. Although the maximum angle of the radiation beam with a loaded substrate is the same as for artificial inclusions, however the antenna gain with stub-loaded H-shaped unit-cells is higher by 3 dB.

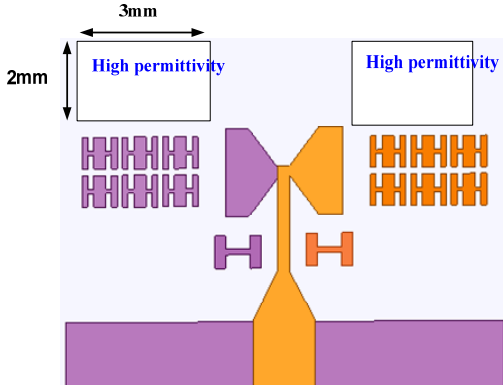


Fig. 8. Configuration of the bow-tie antenna embedded with high dielectric constant material instead of stub-loaded H-shaped unit-cells.

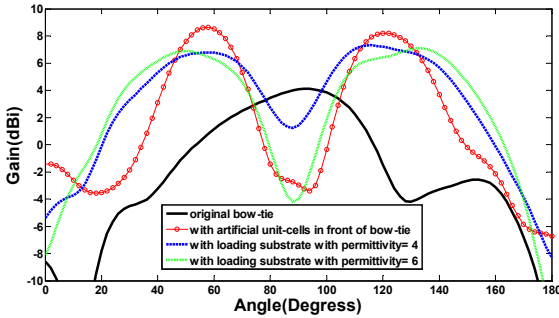


Fig. 9. The radiation patterns of the antenna in the E-plane when loaded with higher dielectric constant substrates.

The dual-beam radiation pattern in the E-plane of the final antenna design at 58, 60 and 62 GHz is plotted in Fig. 10. It is evident that at the three different frequencies, the antenna exhibits maximum radiation at +60 and 120 degrees. Also, the radiation null in the end-fire direction improves significantly from -10 dBi to -30 dBi with increase in frequency from 58 GHz to 62 GHz. Worst case null of -10 dBi at 58 GHz is sufficient for applications such as scanning and millimeter-wave identification systems, as only a tenth of the power is radiated in the undesired direction. The 3 dB beamwidth of the antenna tends to decrease from 32 degrees at 58 GHz to 23

degrees at 62 GHz. The measured gain corresponding to 58, 60, and 63 GHz is 8.7, 8.9, 9.2 dBi, respectively. This variation is tolerable for 60 GHz band systems.

The size of the tilted unit-cell array was obtained from a parametric study. By increasing the number of unit-cells in the  $x$ -direction from  $2 \times 4$  to  $4 \times 4$  attenuates spurious radiation directed towards the end-fire (90 degrees) by 24 dB, as shown in Fig. 11. Increasing the number of unit-cells from  $2 \times 4$  to  $4 \times 4$  in the  $y$ -axis, results in attenuation of the end-fire radiation by 20 dB.

#### IV. EXPERIMENTAL RESULTS

Photograph of the fabricated dual-beam bow-tie antenna with arrays of stub-loaded H-shaped unit-cells is shown in Fig. 12. The proposed antenna was constructed on a Rogers RT5880. A 1.85 mm end-launch Southwest connector was utilized in the measurement of the antenna characteristics. The measured reflection coefficient of the proposed bow-tie antenna is shown in Fig. 13. The magnitude of  $S_{11}$  is better than -10 dB over the frequency band of 55–65 GHz.

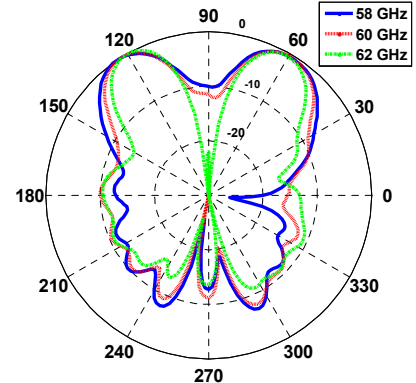


Fig. 10. The normalized radiation patterns of the dual-beam bow-tie antenna in the E-plane ( $xy$ ) at 58, 60, and 62 GHz.

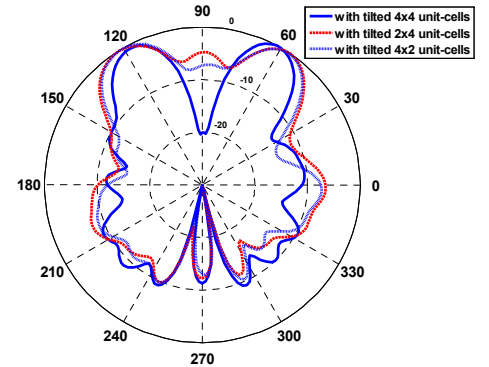


Fig. 11. The normalized radiation patterns of the dual-beam bow-tie antenna in the E-plane ( $xy$ ) obtained by loading different number of tilted unit-cells along the  $x$  and  $y$ -direction at 60 GHz.

It is important to emphasize that the work presented can be regarded as a quasi yagi antenna and, fabrication of this antenna is not complicated as the metamaterial unit-cells can be easily etched in the plane of the antenna using conventional MIC technology. We have used standard manufacturing facilities available to us at the university.

Antenna gain was measured using a compact range anechoic chamber, as shown in Fig.14, where the reference horn antenna is located at the focal point of reflector which converts spherical waves to plane waves directed to the antenna under test. The antenna gain was measured using the comparison method as explained in [16] by measuring the power received by the reference horn antenna and the proposed dual-beam bow-tie antenna, and determining the relative difference in the gain of both antennas. In addition the connector losses were taken into account according to [16]. There is good agreement between simulation and measured results in Fig.15.

The simulated and measured E-plane radiation pattern of the bow-tie antenna with at 58, 60, and 63 GHz are shown in Fig. 15. The measured results show that the main beam direction of the antenna radiates at +60 and 120 degrees with respects to the end-fire direction (90 degrees). In addition, the magnitude of the normalized E-plane radiation in the end-fire direction corresponds to -10 dBi and -15 dBi at 58 and 63 GHz, respectively. The discrepancy between simulation and measured results is attributed to the fabrication tolerance.

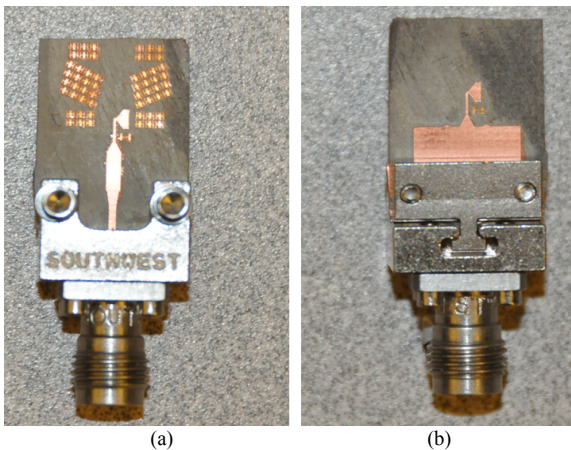


Fig. 12. Photograph of the dual-beam bow-tie antenna loaded with stub-loaded H-shaped unit-cells.

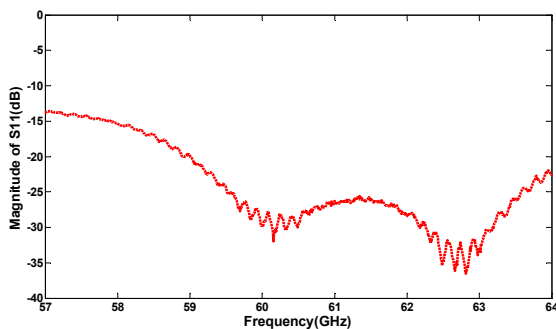


Fig. 13. The measured reflection coefficient of the dual-beam bow-tie antenna.

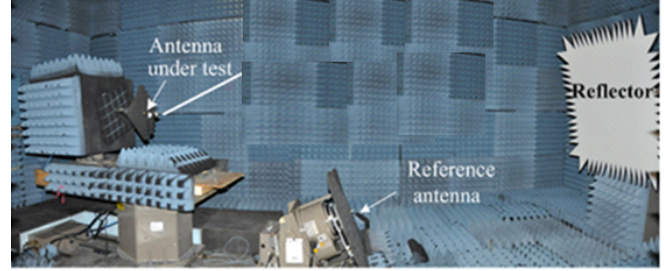


Fig. 14. Equipment setup to measure the radiation patterns and gain of the proposed antenna.

The measured antenna gain at 58 GHz, 60 GHz and 63 GHz are 8.7 dBi, 8.9 dBi and 9.2 dBi, respectively. The proposed antenna is applicable for millimeter-wave indoor communication systems.

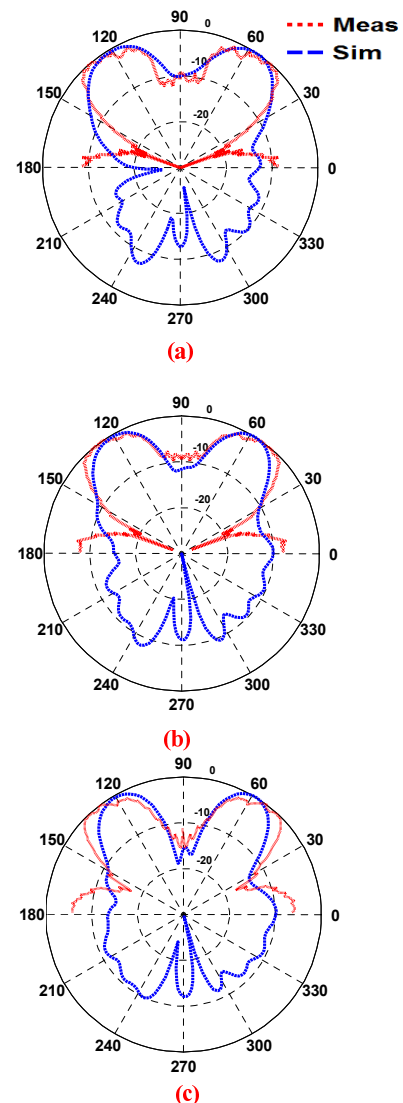


Fig. 15. The normalized radiation patterns of the dual-beam bow-tie antenna using an array of stub-loaded H-shaped unit-cells in the E-plane ( $xy$ ) at: (a) 58 GHz, (b) 60 GHz, and (c) 63 GHz.

## V. CONCLUSION

It has been demonstrated that by artificially manipulating the dielectric constant of the substrate in the end-fire direction of a bow-tie antenna a dual-beam radiation pattern can be realized in the E-plane at 60 GHz. This is achieved using  $4 \times 4$  arrays of metamaterial inclusions implemented using stub-loaded H-shaped unit-cells. By appropriately tilting the inclusions with respect to the bow-tie axis a dual-beam was created at  $+60$  and  $120$  degrees. In addition, it was shown that by including a pair of H-shape resonators in the vicinity of the feed-line and the radiators the back-lobe radiation is reduced and the antenna gain enhanced by 2.66 dB. Inclusion of a further  $2 \times 3$  array of metamaterial inclusions was used to broaden the 3 dB beamwidth of the antenna and enhances its gain by 1 dB. The measured results of the prototype antenna agree well with the simulation results. This antenna exhibits desirable characteristics for indoor communications at 60 GHz.

## REFERENCES

- [1] K. Li, M. Ingram, E. Rausch, "Multi beam antennas for indoor wireless communications," *IEEE Trans. Comm.*, vol. 50, no. 2, Feb. 2002.
- [2] O. Elloumi, J. Song, Y. Ghamri-Doudane, V.C.M. Leung, "IOT/M2M from research to standards: the next steps (Part I)," *IEEE Communications Magazine*, vol.53, issue 9, pp. 8–9, 2015.
- [3] S. Kirthiga, M. Jayakumar, "Performance of dualbeam MIMO for millimeter wave indoor communication systems," *Springer Wireless Personal Communications*, pp 289–307, 2014.
- [4] K. Hosoya, N. Prasad, K. Ramachandran, N. Orihashi, S. Kishimoto, S. Rampath, K. Maruhashi, "Multiple sector ID capture (MIDC): A novel beamforming technique for 60 GHz band multi-Gbps WLAN/PAN systems," *IEEE Trans. on Antennas and Propagation*, vol. 81, no. 1, pp.81–96, Jan. 2015.
- [5] Z.-L. Ma, C.-H. Chan, K.-B.Ng, L.-J. Jiang, "A supercell based dual beam dielectric grating antenna for 60 GHz application," *IEEE Antennas and Propagation & USNC/URSI National Radio Science Meeting*, 2015, pp.643-644.
- [6] A. Lamminen, J. Aurinsalo, J. Säily, T. Karttaavi, J. Francey, T. Bateman, "Dual-circular polarised patch antenna array on LCP for 60 GHz millimetre-wave identification," *European Conference on Antennas and Propagation (EuCAP)*, 2014, pp. 537-541.
- [7] M.-Y. Li, C. T. Rodenbeck, K. Chang, "Millimeter-wave dual-beam scanning microstrip patch antenna arrays fed by dielectric image lines," *IEEE Ant. & Prop. Society Int. Symp.* vol. 2, 2002, pp.196-199.
- [8] S. Raman; G. M. Rebeiz, "Single- and dual-polarized millimeter-wave slot-ring antennas," *IEEE Trans. on Antennas and Propagation*, vol.44, no.11, 1996, pp. 1438-1444.
- [9] R.A. Alhalabi, Y.-C. Chiou, G.M. Rebeiz, "Self-shielded high-efficiency Yagi-Uda antennas for 60 GHz communications," *IEEE Trans. Antennas Propag.*, vol. 59, no. 3, pp. 742–750, 2011.
- [10] S. Jafarloo, M. Bakri-Kassem, M. Fakharzadeh, Z. Sotoodeh, S. Safavi-Naeini, "A wideband CPW-fed planar dielectric tapered antenna with parasitic elements for 60-GHz integrated application," *IEEE Trans. Antennas Propag.*, vol. 62, no. 12, pp. 6010–6018, Dec 2014.
- [11] R.A. Alhalabi, G.M. Rebeiz, "High-gain Yagi-Uda antennas for millimeter-wave switched-beam systems," *IEEE Trans. Antennas Propag.*, vol. 57, no. 11, pp. 3672–3676, Nov. 2009.
- [12] M. Sun, Z.N. Chen, X. Qing, "Gain enhancement of 60-GHz antipodal tapered slot antenna using zero-index metamaterial," *IEEE Trans. Antennas Propag.*, vol. 61, no. 4, pp. 1741–1746, Apr. 2013.
- [13] A. Dadgarpour, B. Zarghooni, B.S. Virdee, T.A. Denidni, "Beam tilting antenna using integrated metamaterial loading," *IEEE Trans. Antennas Propag.*, vol.62, no.5, pp. 2874–2879, May 2014.
- [14] A. Dadgarpour, B. Zarghooni, B.S. Virdee, T.A. Denidni, "Improvement of gain and elevation tilt-angle using metamaterial loading for millimeter-wave applications," *IEEE Ant. Wirel. Prop. Lett.* Early access.
- [15] B. Zarghooni, A. Dadgarpour, T.A. Denidni, "Millimeter-wave antenna using two-sectioned metamaterial medium," *IEEE Ant. and Wireless Propag. Lett.*, Early Access.
- [16] A. Dadgarpour, B. Zarghooni, B.S. Virdee, T.A. Denidni, "Millimeter-wave high-gain SIW end-fire bow-tie antenna," *IEEE Trans. Antennas Propag.*, vol. 63, no. 5, pp. 2337–2342, May. 2015.
- [17] S-G. Kim, K. Chang, "Independently controllable dual-feed dual-beam phased array using piezoelectric transducers," *IEEE Ant. Wirel. Prop. Lett.*, vol.1, pp.81–83, 2002.
- [18] A. Dadgarpour, B. Zarghooni, B.S. Virdee, T.A. Denidni, "Beam deflection using gradient refractive index media for 60 GHz end-fire antenna," *IEEE Trans. Antennas Propag.*, vol. 63, no.8, pp.3768–3774, Aug. 2015.
- [19] M. Al-Hasan, T. Denidni, A.R. Sebak, "60 GHz agile EBG-based antenna with reconfigurable pattern," *IEEE Int. Symp. Ant. & Propag. & USNC/URSI National Radio Science Meeting*, pp.13-14, 2015.
- [20] A. Mehdipour, J.W. Wong, and G.V. Eleftheriades, "Beam-squinting reduction of leaky-wave antennas using Huygens metasurfaces," *IEEE Trans. Antennas Propag.*, vol. 63, no. 3, pp. 978–992, March. 2015.
- [21] W. Cao, W. Hong, Z.N. Chen, B. Zhang, and A. Liu, "Gain enhancement of beam scanning substrate integrated waveguide slot array antennas using a phase-correcting grating cover," *IEEE Trans. Antennas Propag.*, vol.62, no.9, pp. 4584–4591, Sep. 2014.
- [22] T-L. Chen and Y-D. Lin, "Dual-beam microstrip leaky-wave array excited by aperture-coupling method," *IEEE Trans. Antennas Propag.*, vol.51, no.9, pp. 2496–2498, Sep. 2003.
- [23] Z.L. Ma and L.J. Jiang, "One-dimensional triple periodic dual-beam microstrip leaky-wave antenna," *IEEE Antennas & Wireless Propagation Lett.*, vol.14, 2015
- [24] C-C. Hu, C.F. Jou, J-J. Wu, "An aperture-coupled linear microstrip leaky-wave antenna array with two-dimensional dual-beam scanning capability," *IEEE Trans. Ant. Propag.*, vol. 48, no.6, pp. 909–913, Jun. 2000.
- [25] A. Khidre, K-F. Lee, A.Z. Elsherbeni, F. Yang, "Wide band dual-beam u-slot microstrip antenna," *IEEE Trans. Antennas Propag.*, vol.61, no.3, pp. 1415–1418, March. 2013.
- [26] M. Sun, X. Qing, Z.N. Chen, "60-GHz end-fire fan-like antennas with wide beamwidth," *IEEE Trans. Antennas Propag.*, vol. 61, no. 4, pp. 1741–1746, Apr. 2013.
- [27] A. Amadjikpe, D. Choudhury, C. Patterson, B. Lacroix, G. Ponchak, and J. Papapolymerou, "Integrated 60-GHz antenna on multilayer organic package with broadside and end-fire radiation," *IEEE Trans. Microw. Theory Tech.*, vol. 61, no. 1, pp. 303–315, Jan. 2013.
- [28] K.M.K.H. Leong, Y. Qian, and T. Itoh, "Surface wave enhanced broadband planar antenna for wireless applications," *IEEE Microw. Wireless Compon. Lett.*, vol. 11, no. 2, pp. 62–64, Feb. 2001.
- [29] N.G. Alexopoulos, P.B. Katehi, D.B. Rutledge, "Substrate optimization for integrated circuit antennas," *IEEE Trans. Microw. Theory Tech.*, vol. 31, no. 7, pp. 550–557, Jul. 1983.
- [30] Z. Szabó, P.G. Ho, R. Hedge, E.P. Li, "A unique extraction of metamaterial parameters based on Kramers-Kronig relationship," *IEEE Trans. Microw. Theory Tech.*, vol.58, no.10, pp. 2646–2653, Oct. 2010.